Transient temperature and stress fields on bonding small glass pieces to solder glass by laser welding: numerical modelling and experimental validation

Shanwen Zhang[a,*], Min Kong[a], Hong Miao[a], Saim Memon[b], Yanjun Zhang[a], Sixing Liu[a]

[a] College of Mechanical Engineering, Yangzhou University, Jiangsu 225127, China.

[b] London Centre for Energy Engineering, School of Engineering, London South Bank University, 103 Borough Road, London, SE1 0AA, UK.

[*]Corresponding Author: Shanwen Zhang

Address: College of Mechanical Engineering, Yangzhou University, Jiangsu 225127, China

Email: swzhang@yzu.edu.cn

Abstract

Laser welding of transparent materials, including glasses, established in the recent years. This study reports the results of the theoretical with experimental validation to transient temperature and stress fields on bonding small glass pieces to solder glass by laser welding. A 3D finite element model of bonding small glass pieces to solder glass by laser welding is developed and validated with experimental micro-structural analysis. An influence of laser average power and welding speed on the temperature field and stress field during welding is studied. A range of average laser power and welding speed, with a standard of the appropriate temperatures and ultimate stresses of sealing during laser welding, are determined. The results show that in the range of laser average power of 45~75 W and welding speed of 1~2mm/s, the heat source central temperature increases with an increase of laser average power or the decrease of welding speed, and the corresponding maximum temperature exceeds 650°C. The maximum transient thermal stress is calculated to be 152 MPa, it appeared at the boundary of the upper glass interface. The boundary stress at the front end of the heat source and the transient thermal stress at the inflection point are larger than the transient thermal stress at the middle point. The experimental and theoretical results show that the melting layer has excellent morphology and mechanical properties at the average laser power of 65 W and welding speed of 90 mm/min, which is applicable for the bonding of small glass pieces to solder glass by laser welding.

Key words: Laser welding; bonding glass; temperature-induced stresses; finite-element modelling; micro-morphology

1. Introduction

Laser welding technique has the high processing speed, precision, localized bonding and could be used in area bonding with free-shape trajectories (Pablos-Martín et al., 2017). Laser welding of transparent materials, including glasses, has been developed in the past years (Richter S. et al., 2015; Miyamoto I. et al., 2011). Bonding glass by welding is applied in several industrial fields, such as optics, insulation for windows, microelectromechanical systems (MEMS), opto-electronic and medical devices (Shun-Yuan H., et al., 2012; Cao Z. et al., 2013; Memon et al, 2019). Many methods have been developed to bond the two pieces of glass by laser welding. A femtosecond fiber laser with variable repetition rates was focused into borosilicate glass at various pulse energies, repetition rates and traveling velocities for local melting. Results show that the fusion welding of glass by femtosecond laser provided much higher melting and joining efficiencies than existing laser welding of metals (Miyamoto I. et al., 2007). Picosecond laser welding of similar and dissimilar materials based on plasma formation induced by a tightly focused beam from a laser system was studied. The welding of fused silica, borosilicate, and sapphire to a range of materials including borosilicate, fused silica, silicon, copper, aluminum, and stainless steel was demonstrated (Carter R.M. et al., 2014). The laser-based glass sealing joining process for the fuel cell manufacturing is developed by Faidel D. et al. (2010). Laser glass frit sealing for encapsulation of glasses was studied by Kind H. et al. (2014), and the investigation shows that the laser glass frit sealing process was suitable for materials with crucial thermal properties like soda-lime glass. In conclusion, laser welding technique for bonding glass is practicable. To develop this technique, in this paper transient temperature and stress fields on bonding small glass pieces to solder glass by laser welding is investigated by numerical modelling and experimental validation.

In the laser welding process engineering, the distribution of temperature field and stress field are critical factors affecting the quality of bonding small glass pieces to solder glass. It is important to analyze the change of temperature field and stress field in the process of bonding small glass pieces to solder glass by laser welding for designing rational laser process and improving the quality of welding. In this paper, the influence of average laser power and welding speed on the temperature field and stress field in the welding process is discussed. By analyzing the temperature field and stress field, the range of process parameters of average laser power and welding speed is determined. Experiments are also carried out to corroborate the results.

2. Methodology

The heat transfers from heat source to glass solder mainly in the form of convection and radiation, and after the glass solder obtains heat, it mainly transfers to the glass substrate by heat conduction. The main problem of thermal analysis in laser welding process is the temperature field distribution on the joints and its change with time. Therefore, when the temperature field is analyzed by finite element method, heat conduction is the main mode of heat transfer. Fig. 1 shows a calculating flow chart of the laser welding for bonding small glass pieces to solder glass employed in the study.

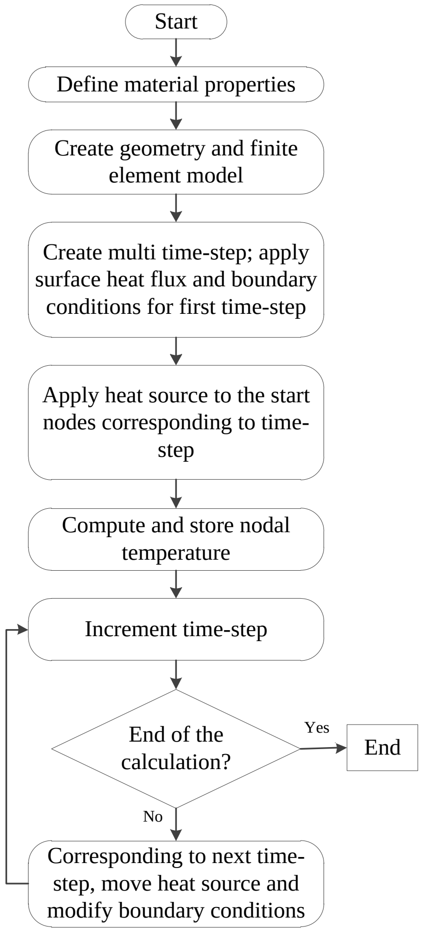

Fig. 1. The flow chart of the laser welding process for bonding small glass pieces to solder glass.

2.1. Numerical modelling approach

The welding process was modeled as a transient thermal analysis. The number of elements heated by the laser is applied with heat source at each time step and the temperature distribution is dependent on the travel speed of the laser. A 3D finite element thermal model developed by using ANSYS/CAE described the model's thermal history in the laser welding process. Transient thermal analysis was performed to determine the temperature history at each position. The heat conduction governing Eq. (1) is as follows.

$$\frac{\partial}{\partial x}\left(\lambda \times \frac{\partial T}{\partial x}\right) + \frac{\partial}{\partial y}\left(\lambda \times \frac{\partial T}{\partial y}\right) + \frac{\partial}{\partial z}\left(\lambda \times \frac{\partial T}{\partial z}\right) + Q = \rho C_p \frac{dT}{dt} \tag{1}$$

Where, ρ is the density of the solder, C_p is the specific heat of the flat glass, λ is the thermal conductivity of the support, T is the dynamic temperatures and t is the time variable. The terms on the left side of the above equation refer to the conductivity heat transfer in the three directions. Q is the energy applied by laser. The terms on the left side of the above equation also refer to transient nature of the heat transfer process. In the numerical modelling calculations, the temperature T_0 began with 250°C.

$$T(x, y, z) = T_0 \tag{2}$$

In the laser welding process, the phase change effects of the melt generation and re-solidification of the low melting point solder is not considered. Whilst the specific material properties, such as density, thermal conductivity and specific heat, are used as inputs in the transient thermal analysis. All surfaces of the flat glass exposed to the air environment were assumed to have lost heat due to free convection and radiation.

According to Rosenthal's Eq. (3), the moving heat source was simulated by applying a constant temperature on the thermal model for a time, which is equal to the distance between the start and the end of the welding divided by the laser travel speed. A user subroutine was written to calculate the position of the laser at a given time to inform a function of its speed (v) and the Gaussian source was assumed as the temperature T_g.

$$\frac{dT}{dt} - \nabla\left(vT\right) - \frac{\lambda}{\rho C_p}\nabla T = \frac{T_g - T_0^{'}}{dt} \tag{3}$$

Where T is the temperature and $T_0^{'}$ is the previous temperature of the position applied by Gaussian source.

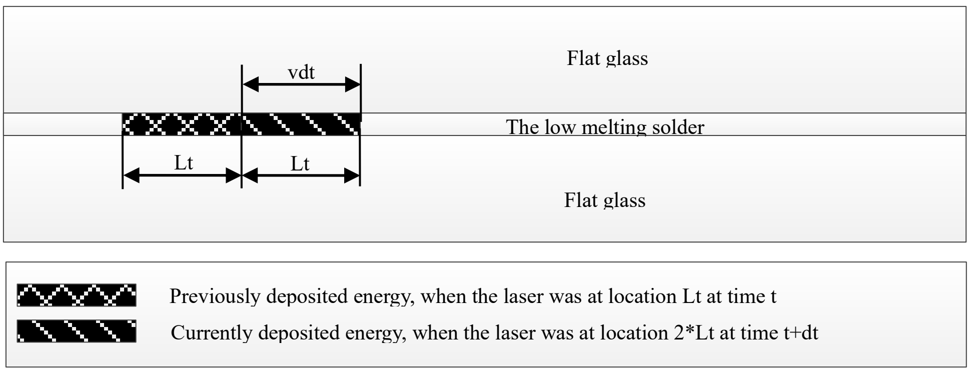

Fig. 2. Schematic illustration of the interaction of the current and previous deposited energy at different times

In the simulation of the laser welding, the interaction of the heat flux between the current and previous Gaussian source follows the schematic in Fig. 2. At time t, the Gaussian source was applied mainly on the solder and the elements at the second location Lt was heated to a transient temperature $T_0^{'}$. At time t+dt, the Gaussian source was moved on the second location Lt and its temperature is heated to T_c.

2.2. Finite element modelling approach

An experimentally and theoretically validated finite element model of Zhang et al. (2011); Shanwen et al. (2014); and Zhang et al. (2017) was employed to model the laser welded edge-seal two pieces of glass sheets. The thickness of upper and lower glass is 4 mm, the thickness of solder is 0.3 mm and the width is 10 mm. The stainless steel support pillar is placed in the middle of two glasses for supporting (Fang et al, 2020) (Memon, 2017). Eight-node three-dimensional solid70 element is used to divide the model. Its geometric model and finite element model are shown in Fig. 4. The overall model size is 70 mm·70 mm·8.3 mm as shown in Fig. 3(a). There are 347965 elements and 358210 nodes. To facilitate the analysis, some analysis points such as Midpoint (MP) and Inflection point (IP) are selected in the model, as shown in Fig. 3(b). Fig. 3 shows the geometric model and finite element mesh of bonding small glass pieces to solder glass pieces.

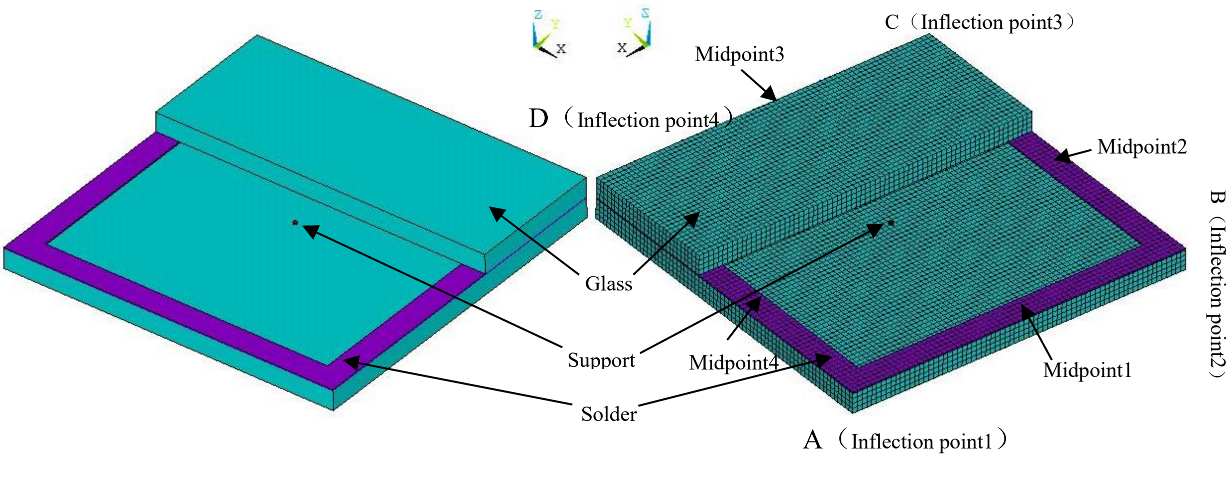

（a）Geometric model （b）Finite element mesh

Fig. 3. (a) Geometric model and (b) finite element mesh of bonding small glass pieces to solder glass for the dimensions of 70 mm·70 mm·8.3 mm.

The flat glass employed in the model and experiment is soda-lime glass, and the solder utilized for laser welding is $PbO\text{-}TiO_2\text{-}SiO_2\text{-}R_xO_y$ powder detailed in Miao et al. (2015). The properties of several materials are shown in Table 1. The natural convective heat transfer coefficient between glass surface and air is modelled to be 5 $Wm^{-2}K^{-1}$, and the preheating temperature of 250℃ is used. In the actual production of laser welded glass pieces, the width of the sealing edge is fixed, so the diameter of the spot acting on the solder surface is constant and the diameter is 10 mm, so the influence of average laser power and welding speed on the temperature field are analyzed in this paper. The average laser power ranges from 45 to 75 W, the welding speed ranges from 1 to 2 mm/s, and the welding path is A-B-C-D-A.

Table 1

Material properties of the components employed in the finite-element modelling of bonding small glass pieces to solder glass.

Material	Density kgm^{-3}	Sepcific heat capacity $Jkg^{-1}K^{-1}$	Thermal conductivity $Wm^{-1}K^{-1}$	Elastic modulus （MPa）	CTE （K^{-1}）	Poisson's ratio
Glass	2460	790	0.75	6.89×10^{4}	10.2×10^{-6}	0.23
Solder	3130	130	35	1.4×10^{4}	9.1×10^{-6}	0.4
Support	7800	406	18	2×10^{5}	1.1×10^{-5}	0.28

During the welding process, the laser energy is loaded on the glass surface in the form of heat flux, and moves at a certain speed. The ANSYS APDL is used to establish a moving heat source, which provides heat load input at different times and locations, and simulates the temperature distribution in the laser welding process. Because the welding process is very complicated, the boundary condition is assumed for finding the reasonable laser welding parameters and the convenience of calculation:

- The thermophysical parameters of material are constant and do not change with temperature;
- Homogeneous and isotropic material；
- Heat transfers through conduction on the laser welded edge-seal;
- Neglecting the heat loss caused by convection and heat radiation on the boundary；
- There was no serious vaporization and geometric deformation in the calculation process;
- The glass absorbs very little laser energy and it's zero. The solder absorbs heat and melts to connect the glasses. Because the thickness of the solder is 0.3 mm, the heat transfer is very quickly and the glass temperature field on both sides of the solder could be symmetrical. In fact, laser would be absorbed by the top glass and lower as well, and that will heat the upper/lower glass and the solder. This will be good for reduction of the thermal stresses. The assumption we made is the attempt to predict the laser welding at its comparative stage.

In the FEM model, the point heat source and line heat source can be used as the analytical solution of temperature field in laser welding. The Gauss surface heat source model is more practical than point heat source and line heat source. The heat flow distribution function of Gauss surface heat source model (Mahmood et al. 2007) (Memon et al, 2018) utilized in finite-element model is given in Eq. (4).

$$I(x,y,z,t)=\frac{P}{\pi d^2}\cdot\eta\cdot\exp\left(-2\frac{(x-vt)^2+y^2}{d^2}\right)\delta(z) \quad (4)$$

Where, P is the average laser power, d is the diameter of the spot on the surface of the material, and η is the thermal efficiency of the heat source, 0.8 and v is the welding speed and $\delta(z)$ the impact function.

3. Results and analysis

3.1. Transient temperature field analysis of laser welded edge-seal

Fig. 4 shows the temperature curve along the thickness direction of the heat source center at different times, when P=60 W and v=1.5 mm/s. In Fig. 5, the glass temperature field on both sides of the solder is symmetrical due to the heat source acts directly on the solder. Whilst, the glass is heated through heat conduction, the temperature peak value is on the solder layer. Farther away from the interface between the solder and the glass, the temperature is lowering down. In order to visually display the temperature field distribution at the interface between solder and glass, only the solder layer and the lower glass were taken for transient temperature field analysis.

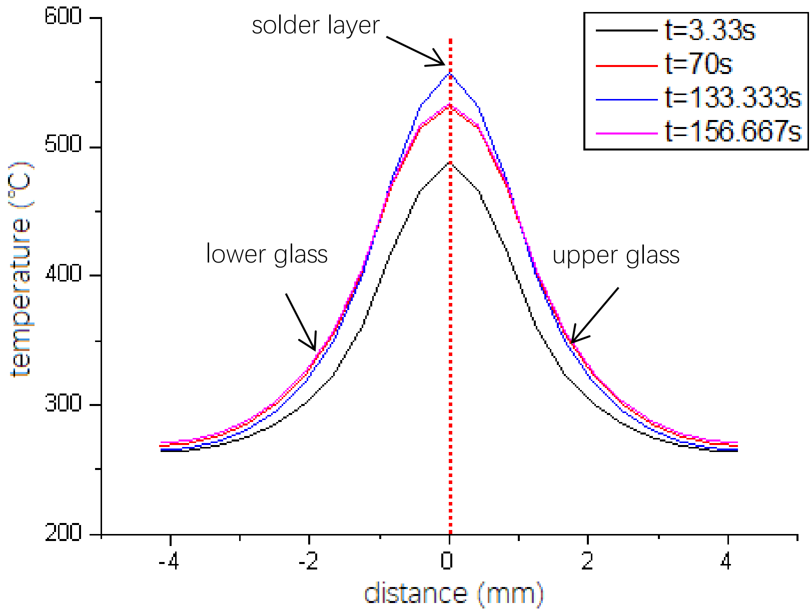

Fig. 4. The transient temperature fields showing heat source center along thickness direction at different times with P=60 W and v=1.5 mm/s.

Fig. 5 shows the temperature distribution of P=60 W, v=1.5 mm/s at different times. In Fig. 5, the maximum temperature of the transient temperature field appears in the center of the heat source. When the heat source reaches a certain point, the instantaneous temperature of the point increases rapidly. After leaving the point, it decreases rapidly to become stable. The instantaneous temperature at the inflection point is higher than the instantaneous temperature at the intermediate stage, mainly because the thermal accumulation is easy to occur at the inflection point. The temperature of the outer edge-sealing solder is higher than that of the inner because of the thermal accumulation at the boundary. The heat affected zones on the welding path are similar during the whole welding process.

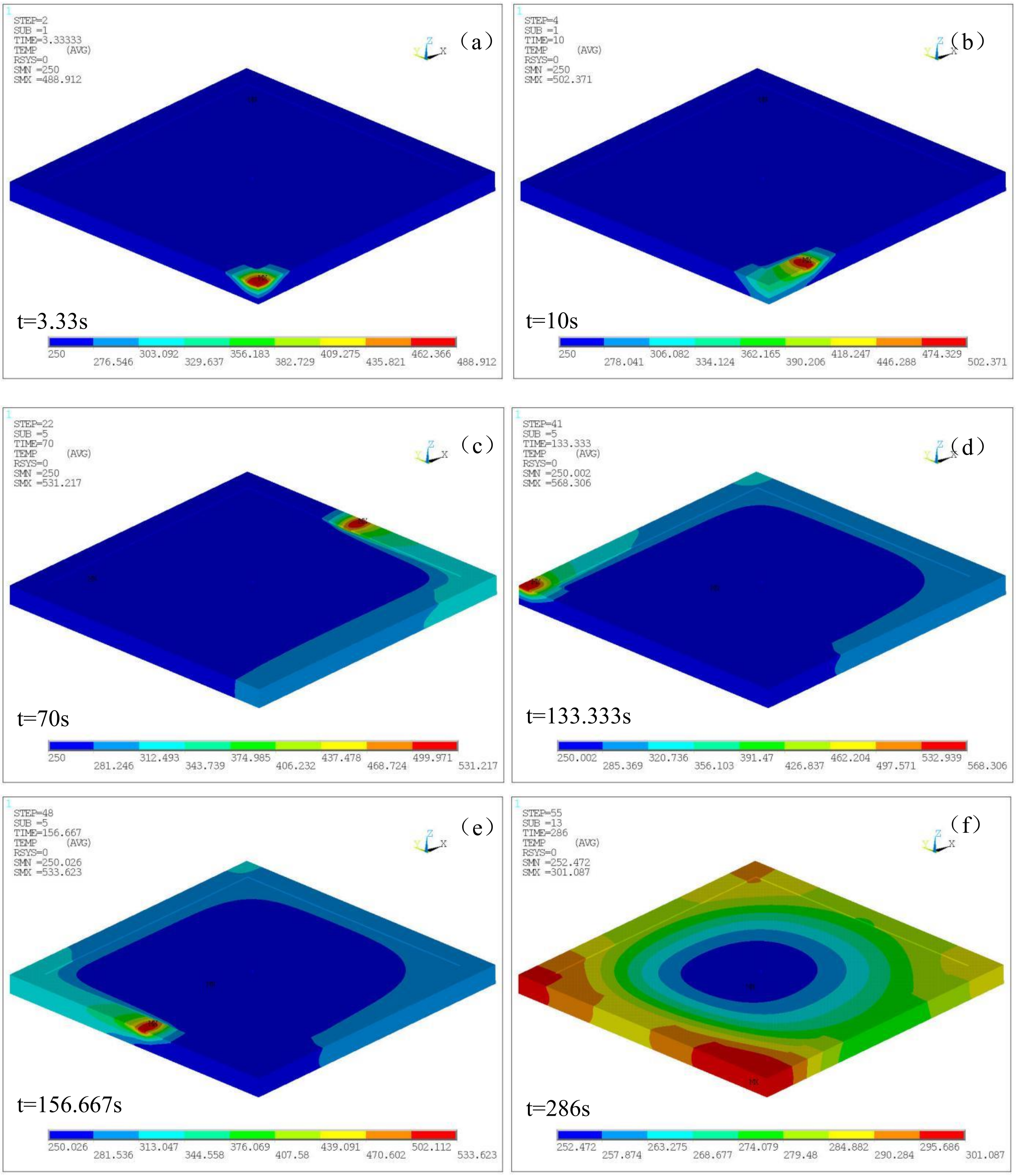

Fig. 5. The temperature fields distribution at the transient time with P=60W and v=1.5 mm/s.

Fig. 6 shows the temperature-time curves at different nodes when P= 60 W and v=1.5 mm/s. In Fig. 6, the temperature curve of each point is basically the same, but there is a time difference. Before the heat source reaches the point, the point absorbs laser energy rapidly and converts it into heat energy, and the temperature increases sharply. When the heat source just leaves the point, because the temperature gradient between the point and the surrounding material is large, the heat diffuses and transmits rapidly to the surrounding material, and the temperature decreases rapidly. When the surrounding material approaches the heat balance with the point, the temperature slowly decreased. This process can clearly see the characteristics of laser local rapid heating and cooling, and the cooling process of each point is much slower than that of heating process. The initial maximum temperature at midpoint 1 (MP1) and inflection point 1 (IP1) are slightly lower than that at other points, mainly because the quasi-steady state has not yet been reached at this time. When the quasi-steady state is reached, the change process of each point is basically the same.

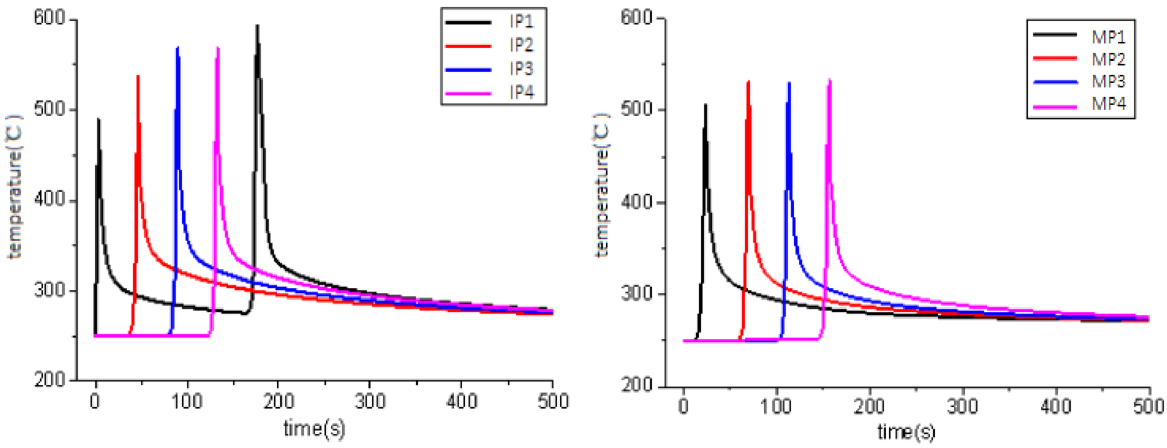

Fig. 6. The temperature/time curves at different nodes with P=60W and *v*=1.5mm/s showing the inflection points (IP) midpoints (MP).

3.2. The effect of laser average power on temperature fields

Fig. 7 shows the temperature distribution when the heat source steps along the midpoint 2 (MP2) under various average laser powers. By adjusting the average laser power, no effect on the distribution of the temperature fields is observed, but when the average laser power increases, the maximum temperature in the welding area increases. The average laser power determines the power density of each point. When the laser power is insignificant, the power density is exceedingly small, the energy absorbed by solder becomes small whilst the temperature of the laser welding area is lower at the constant time. When the laser power is larger, the energy absorbed by solder is larger and the temperature of laser welding area is higher.

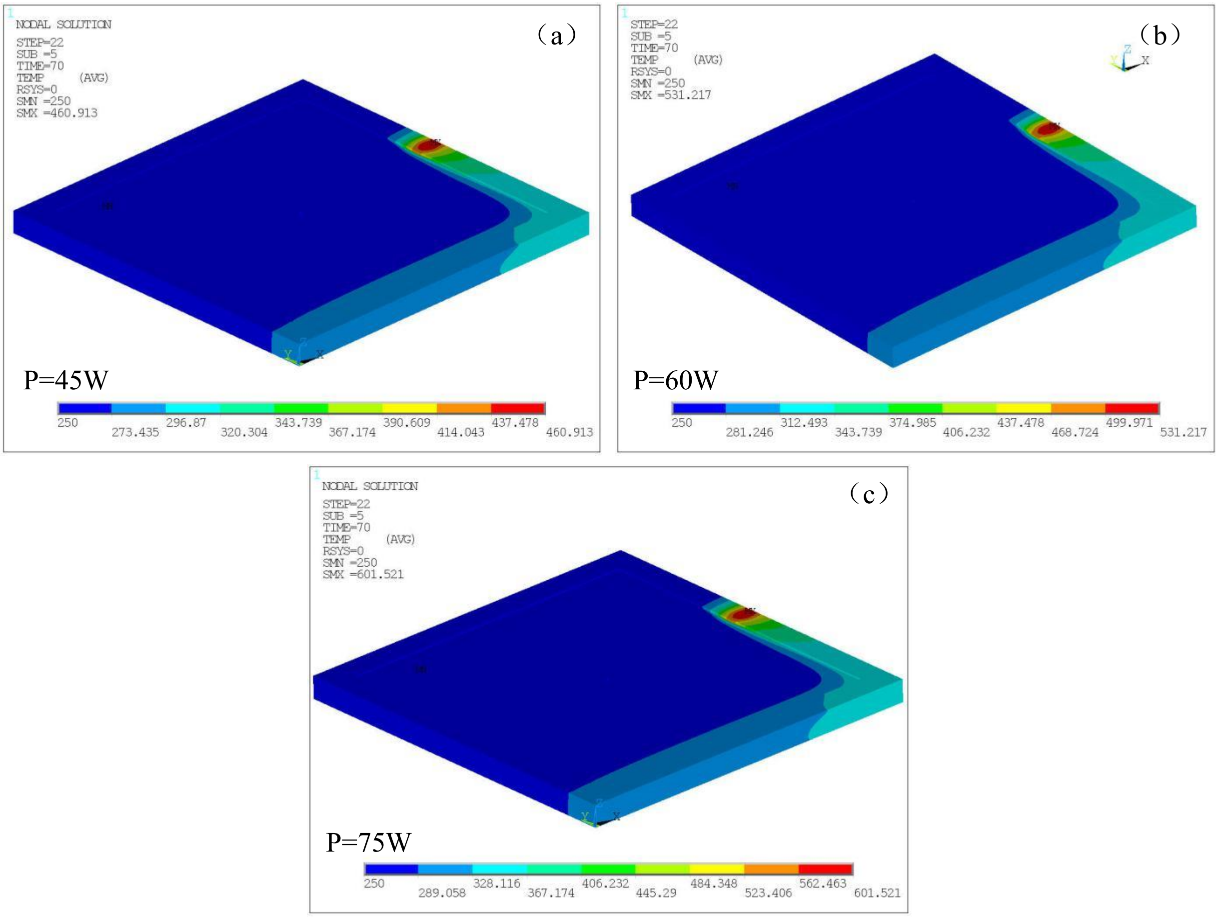

Fig. 7. The temperature distribution of the heat source moving along the midpoint 2 (MP2) under different laser average powers.

Fig. 8 illustrates the temperature-time trajectory of the heat source center under particular average laser powers. The results show changing the average laser power can only change the maximum temperature of the heat source center, and the trend of temperature change is the same during the whole welding process. When the loading time of the laser source is short, the temperature rises rapidly but unsteadily due to a rapid heat effect from heat source radiation; when the heat source moves, the temperature rises gradually in AB section; when the heat source reaches the glass "L" inflection point, the temperature rises rapidly and shows the heat accumulation effect obviously. Because the heat at the end point just has one-way conduction, heat cannot be released in time, and accumulates at the endpoint which makes the temperature rise continuously. When the heat source moves out of the inflection point, the temperature drops rapidly to a stable state. The temperature field of the whole welding process is as follows: AB section is in the heating stage, BC and CD section are in the stable stage, the first half of DA section is in the stable stage, and the temperature of the second half slightly increases because of the influence of the secondary heating of the heat source near point A.

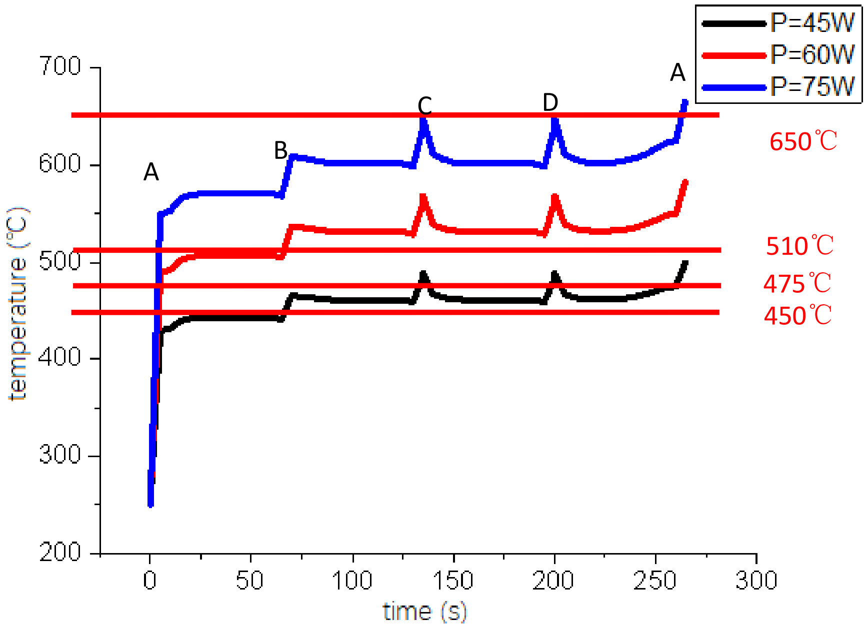

Fig. 8. The temperature-time curves of heat source centers at different average laser powers showing AB section is in the heating stage, BC and CD section are in the stable stage, the first half of DA section is in the stable stage and the temperature of the second half of DA section is slightly increased due to the influence of the secondary heating of the heat source near point A.

The results show when the average laser power is lower than 45 W, the input energy of heat source is low, and the temperature at the connection interface will be lower than 450°C, which is not conducive to or cannot form a better joint. When the average laser power is higher than 75 W, the input energy of heat source is high, and the temperature at the connection interface will be higher than 650°C, if the heat cannot be released in time at the joint, and local overheating may also occur. Because the liquidus temperature of solder is 450°C, the suitable sealing temperature is 475~510°C, and the softening temperature of glass is 650°C, if the temperature is 475~510°C, good joints can be formed in this region. Combining with Fig. 8, when the average laser power is 45 W, the temperature of the heat source center is lower than 475 °C, and the solder may not melt completely; when the average laser power is 75 W, the overall temperature is about 600°C, which may cause over-burning of solder in the welding process, and the glass may be impaired if the temperature of some points is higher than the glass softening temperature of 650°C. When the average laser power is 60 W, the overall temperature is about 530°C, and the suitable sealing temperature near the solder is much lower than the glass softening temperature, which is the closest to the optimal temperature. Therefore, the average laser power of 60 W is selected as a quantitative study to study the influence of welding speed on temperature field.

3.3. The impact of laser welding speed on transient temperature fields

Fig.9 shows the temperature distribution when the heat source moves to the midpoint 2 (MP2) at different welding speeds. The results show that the time of laser radiation on the material surface is related to the welding speed. With the increase of welding speed, the maximum temperature in the welding area decreases gradually with the increase of the time of laser radiation. When the welding speed is lower than 1 mm/s, the time of laser radiation is long, the energy absorbed by the solder is more, and the temperature of the welding area is relatively high; the welding speed is higher than 2 mm/s, the energy absorbed by the solder is less, and the temperature is lower.

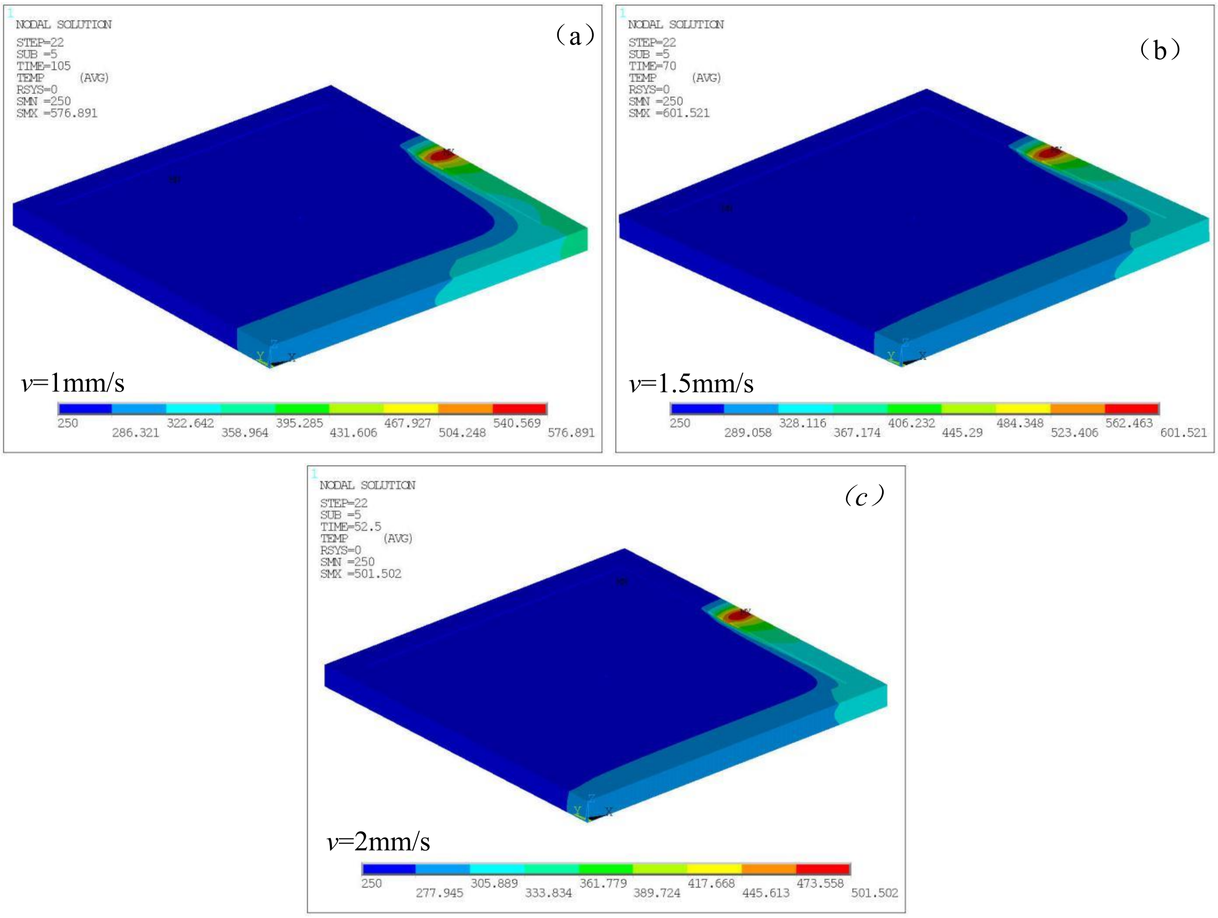

Fig. 9. The temperature distribution when the heat source moves along the midpoint 2 (MP2) at different welding speeds.

The evaluated results show that the scanning speed is lower than 1 mm/s, the interface absorbs lots of heat, and the joint temperature is as high as 650°C, which may cause local overheating and is not conducive to the formation of good joint; the scanning speed is higher than 2 mm/s, the interface absorbs insufficient heat, and the joint temperature is as low as 450°C and the actual sealing area cannot be formed. Fig. 10 is the temperature-time curve of the heat source center at different welding speeds. The results show that when the welding speed is 1 mm/s, when the heat source is stable, the temperature of the heat source center is about 576°C. Due to secondary heating, The temperature at point A is higher than the glass softening temperature of 650°C, and the overall temperature is higher; when the welding speed is 2 mm/s, the temperature in AB section is lower than 475°C, which may lead to the uneven melting of the solder in AB section; when the welding speed is 1.5 mm/s, it is the closest to the ideal temperature.

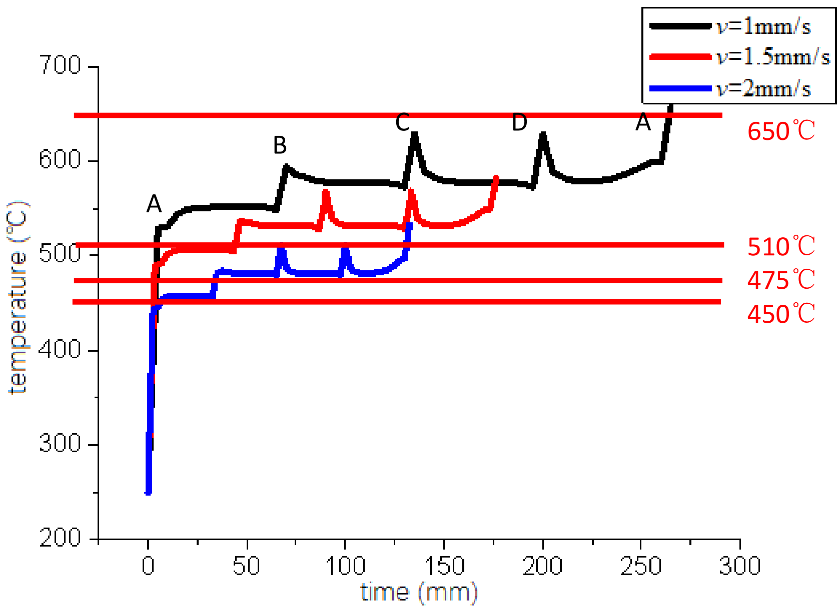

Fig. 10. The temperature/time curves of heat source center at different welding speeds.

3.4. Stress fields analysis on laser welded edge-seal

Fig. 11 shows the stress distribution at different times when P=60 W and v=1.5 mm/s. The thermal stress distribution of upper and lower glass is approximately symmetrical during the whole welding process. When the heat source reaches a certain point, the transient thermal stress at this point increases rapidly, and then decreases rapidly to a stable level after leaving the point. The maximum transient thermal stress occurs at the interface boundary of upper glass. The boundary stress of the front end of the heat source is larger. The transient thermal stress at the inflection point is larger than that at the intermediate stage, mainly because the thermal accumulation easily produces at the inflection point and then causes stress concentration, resulting in the sudden increase of the thermal stress at the inflection point. When the laser welding is finished and thermal energy is removed, the thermal stress decreases and the whole thermal stress field are symmetrically distributed.

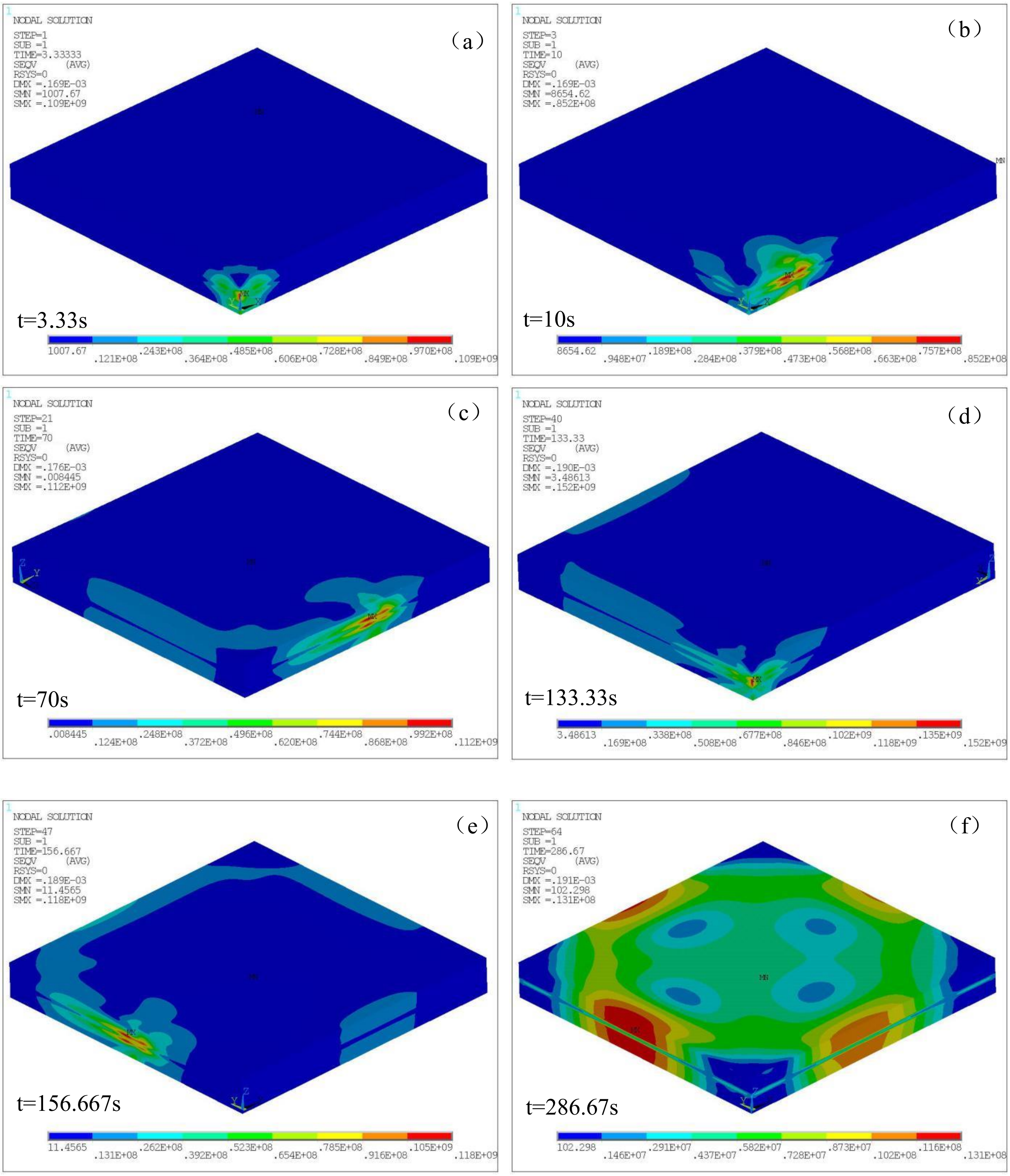

Fig. 11. The stress fields distribution of laser welded edge-seal at different times at P=60 W and *v*=1.5 mm/s.

Fig. 12 shows the variation curve of maximum transient thermal stress with moving distance under different process parameters. Changing the average laser power or welding speed has no effect on the trend of transient thermal stress at each point. The variation range of thermal stress at inflection point is large, and it is parabolic in the intermediate stage, and the thermal stress in AB section is higher than that in other stages. From the analysis of temperature field above, it can be seen that AB section is in the heating stage. Compared with AB section, the temperature gradient is low and the thermal stress is low.

Due to the nature of glass brittleness, when the thermal stress exceeds its limit stress of 140 MPa (Memon et al, 2019), it is easier to cause thermal cracking of the glass in the laser welding process, resulting in sealing failure. Combining with Fig.13, when P = 75W, v = 1.5 mm/s and P = 60 W, v = 1 mm/s, most of the transient thermal stresses in BC, CD and DA sections exceed their limit stresses of 140 MPa, and when P = 60 W, v = 1.5 mm/s, the transient thermal stresses of 152 MPa only exceeds 140 MPa at inflection point.

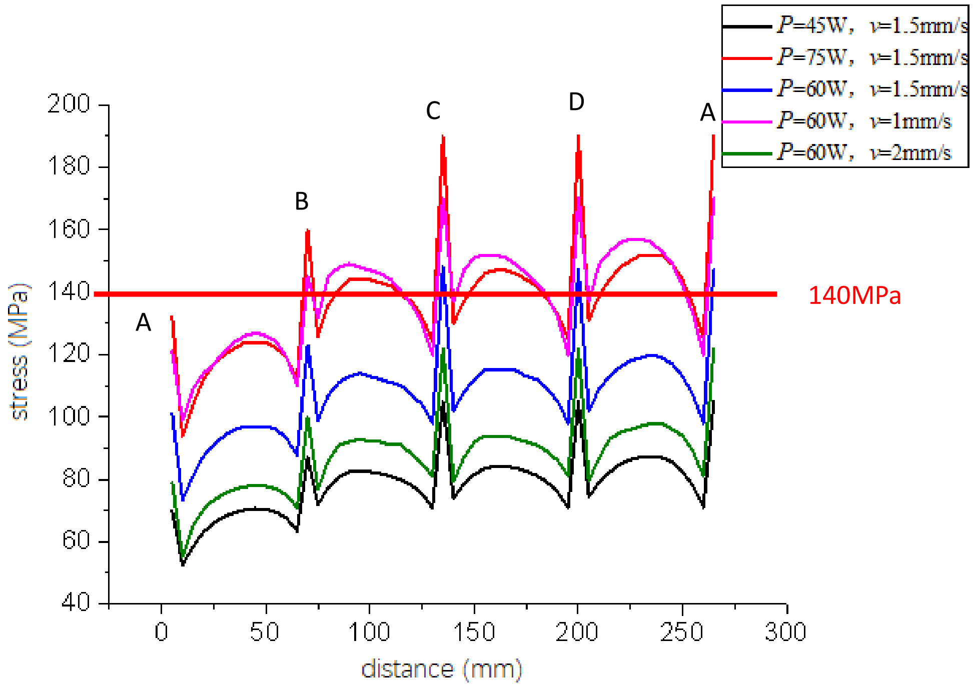

Fig. 12. The stress pressure/distance curves showing maximum transient thermal stress with moving distance under different laser powers and welding speeds.

In the process of laser rapid heating and cooling, the temperature gradient will be formed inside the material due to the inconsistency of heat dissipation speed between the surface and the interior of the material. Since thermal expansion performance of solder differs from glass, the transformation of solder from melting state to solidification state will result in thermal residual stress at the edge of bonding small glass pieces, which will make it the most vulnerable part of the whole structure. Fig. 13 shows the residual stress distribution at the whole and interface after cooling to room temperature at P=60 W and v=1.5 mm/s. Fig.13(a) shows that the residual stress distribution of upper and lower glass is symmetrical. At the interface, as shown in Fig. 13(b), the residual stress distribution around the sealing edge is similar. Because the thermal conductivity of solder is small, it is a poor conductor of heat. Therefore, the greater the temperature gradient in the cooling process, the greater the residual stress in the solder layer than that in the glass.

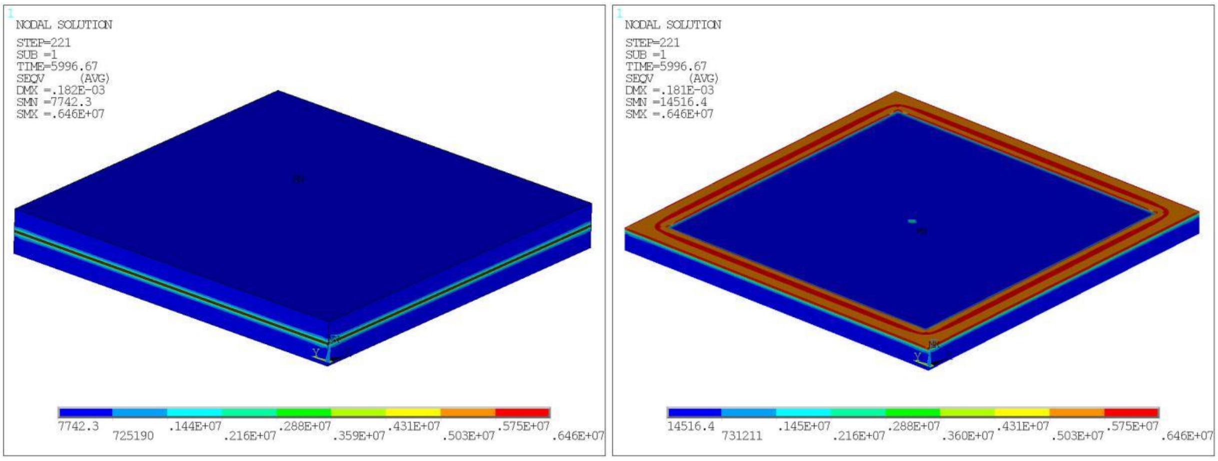

（a）Residual stress distribution （b）Residual stress distribution at interface

Fig. 13. The residual stress distribution at the whole and interface after welding at P=60W and *v*=1.5mm/s.

Table 2 shows the maximum residual stress of sealing edge under different process parameters. The results show that the process parameters have little influence on the maximum residual stress of bonding small glass pieces. The maximum residual stress is about 6.46 MPa, which does not exceed 10 MPa allowed by the residual stress of bonding small glass pieces, meeting the requirements.

Table 2

Maximum residual stress of the laser welded edge seal under different process parameters.

Average laser power（W）	Welding speed（mm/s）	Residual stress（MPa）
45	1.5	6.46
75	1.5	6.47
60	1.5	6.46
60	1	6.47
60	2	6.46

Throughout the analysis of the temperature and stress distributions in the welding process, it can be seen that the thermal stress is lower than the ultimate stress when the laser power is 45 W and the welding speed is 1.5 mm/s, but the maximum temperature of the heat source in some areas is lower than 450°C of the liquidus, so the sealing joint cannot be formed; when the average laser power is 75 W, the maximum temperature and thermal stress of the heat source in some areas exceed their allowable values. When the average laser power is 60 W and the welding speed is 1 mm/s, the maximum temperature and thermal stress of the heat source in some areas exceed the allowable values. When the average laser power is 60 W and the welding speed is 2 mm/s, the thermal stress is lower than the ultimate stress, but some areas may not melt completely. Therefore, the suitable process parameters may be between the average laser power of 45~75 W and the welding speed of 1~2 mm/s.

3.5. Experimental validation

In order to verify the correctness of the numerical simulation results, laser sealing experiments were carried out. The effects of average laser power and welding speed on the micro-morphology of the sealing layer were studied. The mechanical properties of the sealing edge were measured by experiments, and the optimal technological parameters were found by comparison. The material, welding speed, average laser power and other process parameters used are consistent with the computer simulation.

3.5.1. Experimental preparation and instrument description

The mechanical properties of bonding small glass pieces to solder glass by laser welding are tested, and the preparation method of the sample is as follows: 20 mm·20 mm glass solder is applied on the center of a 120 mm·20 mm·4 mm glass bar; another glass bar of the same size is placed on the solder and the two glass bars are perpendicular each other; the prepared sample is put on the laser platform, and after the laser welding and cooling, the two glass bars are bonded together by solder. In this test, we selected HGL-LCY300 Nd: YAG laser, as shown in Fig. 14.

Fig. 14. HGL-LCY300 Nd: YAG laser welding system

Micro-morphology observation: the micro-morphology of the melting layer under different process parameters is observed by Zeiss-soupra55 field emission scanning electron microscope. The test instrument is shown in Fig. 15.

Fig. 15. Zeiss-soupra55 field emission scanning electron microscope

Hardness test: the hardness of samples under different process parameters is tested by MHV-1000 Vickers hardness tester. 20 test points are taken for each sample and then the average value is obtained. The test conditions are as follows: the load is 200g, the holding time is 15s, the average value is taken after multi-point measurement, and the hardness test position and test instrument are shown in Fig. 16.

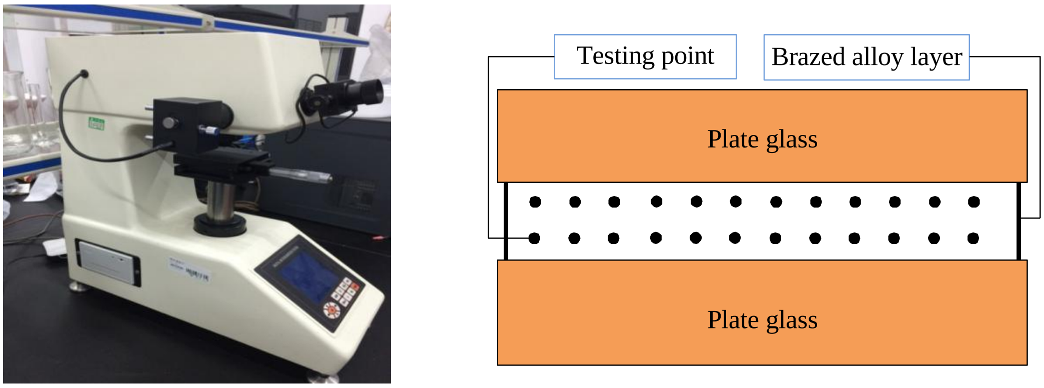

（a）MHV-1000 Vickers hardness tester （b）test position

Fig. 16. Hardness test position and test instrument

Sealing strength test: the edge sealing strength of bonding small glass pieces to solder glass by laser welding includes the tensile strength and shear strength of the edge sealing interface. The tensile strength and shear strength of the edge sealing interface shall be in accordance with *ISO13124 fine ceramics (advanced ceramics, advanced technical ceramics)-Test Method for interface bond strength of ceramics materials*.

When measuring the tensile strength, as shown in Fig. 17, place the cross sample in the fixture to ensure that there is no friction between the sample and the fixture. In order to make the contact between the indenter and the sample even, a piece of soft tape should be bonded on the bottom surface of the upper indenter. The width of the indenter must be the same as the width of the sample, and the lower surface of the indenter should be parallel to the horizontal column below. Load is applied at the speed of 0.2 mm/min until the interface is disconnected, and the maximum load value at the time of fracture is recorded. The average value is taken after measuring each group of process parameters for 5 times. The tensile strength is calculated according to Eq. (5):

$$\sigma_t = \frac{P_t}{A_1} \tag{5}$$

Where P_t is the fracture load, and A_1 is the bond area in the tensile test.

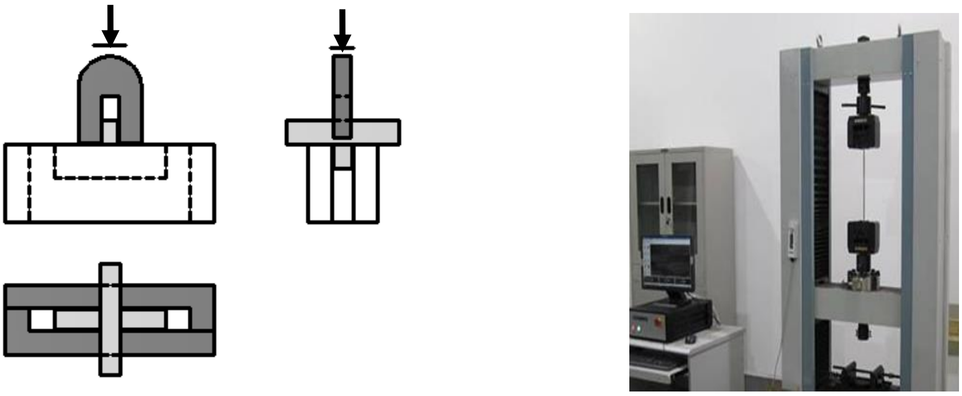

（a） Schematic diagram of tensile strength test （b） Electronic universal testing machine

Fig. 17. Hardness test position and test instrument

When measuring the shear strength, as shown in Fig. 18, place the sample in the fixture. In order to make the contact between the indenter and the sample even, a piece of soft tape shall be bonded at the bottom of the upper indenter. Load is applied at the speed of 0.2 mm/min until the interface is disconnected, and the maximum load value at the time of fracture is recorded. The average value is taken after measuring each group of process parameters for 5 times. The shear strength is calculated according to Eq. (6):

$$\tau = \frac{P_t}{A_2} \tag{6}$$

Where P_t is the fracture load, and A_2 is the bond area in the shear test.

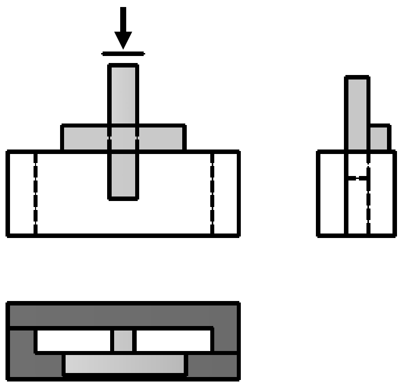

Fig. 18. Schematic diagram of interface shear strength test

3.5.2. Experimental results

Fig. 19 shows the micro-morphology of the melting layer under different average laser powers at welding speed of 90 mm/min. The higher the average laser power, the more fully the solder melts, the better the solder spreads, the smoother the surface of the melting layer and the higher the density. When the average laser power is 75 W, there are many micro-cracks on the surface of the melting layer. The causes of the cracks may be as follows: due to the high input energy of laser, the solder melts completely, the sealing layer is smooth and compact after solidification, while the liquid solder shrinks during cooling process, resulting in tensile stress in the sealing layer, which pulls the solidified weld open, and when there is not enough liquid solder to supplement, cracks will be formed. By analyzing the above test data, when the average power is 65 W, the morphology of the melting layer is better and the welding quality is better.

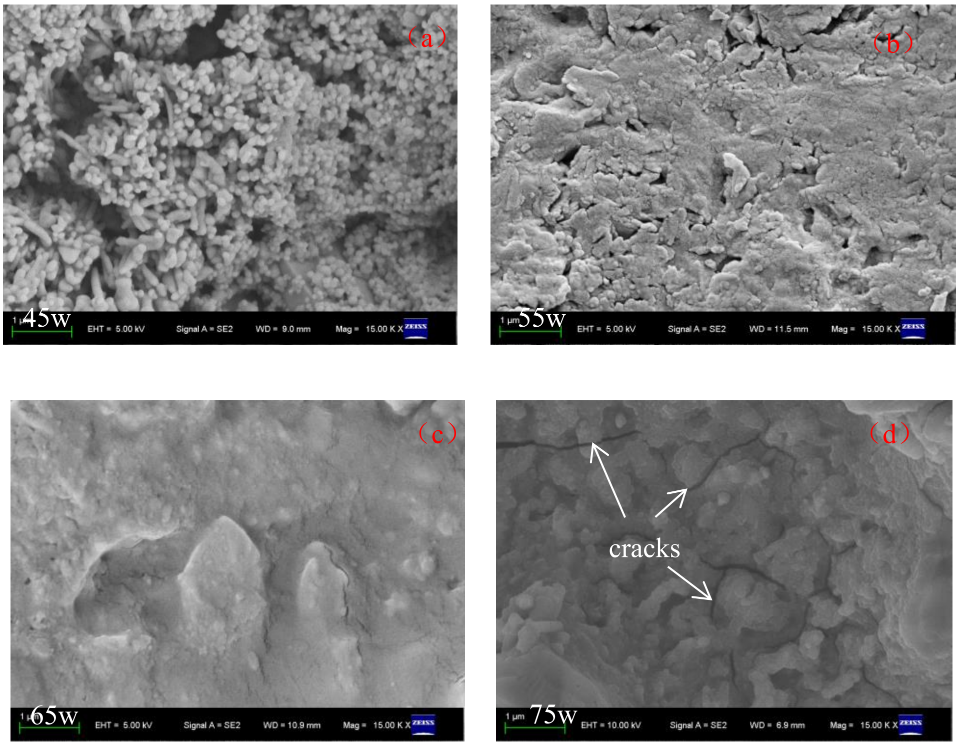

Fig. 19. Scanning electron microscopic morphology of laser welded layer at different laser average powers

Table 3 shows the hardness, tensile strength and shear strength of the sealing layer under different average laser powers at welding speed of 90 mm/min. It can be seen that with the increase of average laser power, the melting amount of the melting layer increases, the liquid phase structure of the sealing layer increases gradually. The sealing layer is completely filled with solder and the bonding effect among particles is good. Therefore, the hardness of the sealing layer is getting higher and higher, and the tensile strength and shear strength are also higher. Because there are a lot of tiny cracks in the melting layer when the average laser power is 75 W, the fracture tendency of the sealing layer will be aggravated during the stretching process, and the tensile strength and shear strength will be reduced. By analyzing the above test data, when the average power is 65 W, the mechanical properties are better and the welding quality is better.

Table 3

Hardness, tensile strength and shear strength of sealing layer under different laser average powers

Average laser power （W）	Hardness （HV）	Tensile stress （N）	Tensile strength （MPa）	Shear stress （N）	Shear strength （MPa）
45	430.26	203.4	0.51	1452	3.63
55	432.47	252	0.63	1737	4.34
65	444.74	261.3	0.65	1753	4.38
75	425.95	168.3	0.42	927	2.32

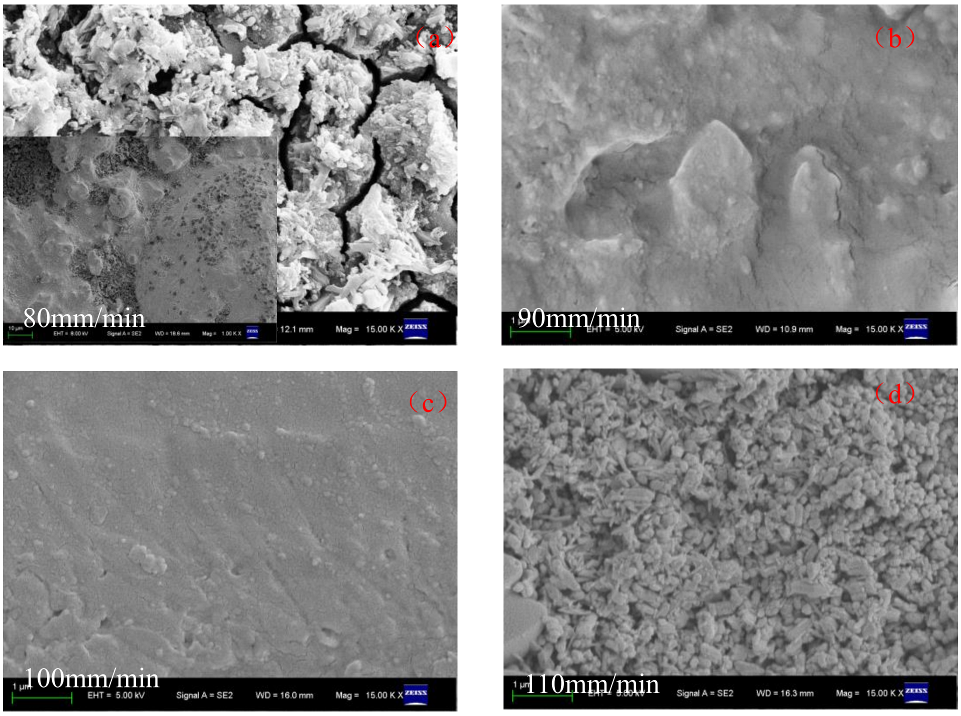

Fig. 20. Scanning electron microscopic morphology of the laser welded layer at different welding speeds.

Fig. 20 shows the micro-morphology of the melting layer at different welding speeds when the average laser power is 65 W. The smaller the welding speed, the more sufficient the solder melts. When the welding speed is 80 mm/min, because the laser input energy is too large, the sealing layer produces large thermal stress, and there are many connected cracks in the melting layer. When the magnification factor is reduced, the internal zones of the sealing layer are seriously burned due to the excessive laser input energy; when the welding speed is increased to 90 mm/min and 100 mm/min, the sealing layer is smooth and compact; when the welding speed is 110 mm/min, the laser input energy is low, and the melting layer solder is not fully melted. By analyzing the above experimental data, the morphology of the melting layer is good and the welding quality is good when the welding speed is 90 mm/min and 100 mm/min .

Table 4 shows the hardness, tensile strength and shear strength of the sealing layer at different welding speeds when the average laser power is 65 W. The hardness, tensile strength and shear strength of the sealing layer first increase and then decrease with the increase of welding speed. When the welding speed is 90 mm/min, the peak value is reached. When welding speed is 90~100 mm/min, the sealing layer spreads well and the density of melting layer is high, so its mechanical properties are relatively high. Due to the existence of large cracks in the sealing layer at 80 mm/min welding speed, which will aggravate its fracture tendency, its tensile strength and shear strength will be very low. When welding speed is 110 mm/min, there are a large number of unmelted powders in the sealing layer, and the bonding effect among particles is poor, so the mechanical properties of the sealing layer will decrease with the increase of welding speed. By analyzing the above test data, the mechanical properties are better and the welding quality is better when the welding speed is 90 mm/min, which can be chosen as optimal parameter.

Table 4

Hardness, tensile strength and shear strength of sealing layer at different welding speeds

Welding speed （mm/min）	Hardness （HV）	Tensile stress （N）	Tensile strength （MPa）	Stear stress （N）	Stear strength （MPa）
80	437.79	152.4	0.38	783	1.96
90	444.74	261.3	0.65	1753	4.38
100	430.15	254.7	0.64	1536	3.84
110	421.54	196.5	0.49	918	2.30

Therefore, when the average laser power is 65 W and the welding speed is 90 mm/min, the melting layer has better morphology and quality of sealing layer, which is an optimal set of process parameters.

In the range of average laser power 45~75 W and welding speed 1~2 mm/s, the melting layer has good morphology, which is suitable for bonding small glass pieces to solder glass. Moreover, properly increasing the average laser power will help to improve the micro-morphology of the sealing layer. Excessive average power will cause cracks in the sealing layer, aggravate the fracture tendency of the sealing layer and reduce its mechanical properties; the low welding speed will cause the solder to burn over and produce a large number of connecting cracks in the sealing layer. The high welding speed will cause the solder to melt unevenly, the bonding effect of solder particles is poor, and the mechanical properties of solder particles are poor.

5 Conclusions

The control mechanisms of laser power level and laser welding rate was analysed for bonding small glass pieces to solder glass with laser welding method. Following are the main conclusions.

(1) The maximum temperature of transient temperature fields occurs at the center of the heat source; the temperature gradient of the front end of the heat source is larger than that of the back end of the heat source; the temperature of outer edge-sealing solder is higher than the inner one; the temperature field of the whole welding process is as follows: AB section is in the heating stage; BC and CD section are in the stable stage; the first half of DA section is in the stable stage; the second half of DA section is slightly higher due to the influence of the secondary heating of heat source near point A; and the heat accumulation effect is easy to occur at the "L" inflection point, and the temperature is higher.

(2) Changing the average laser power or welding speed can only change the maximum temperature of the heat source center. The temperature change trend is the same throughout the welding process. The temperature of the heat source center increases with the increase of the average laser power or the decrease of welding speed, and the maximum temperature exceeds 650℃.

(3) The maximum transient thermal stress is 152 MPa, which occurs at the interface boundary of the upper glass. The boundary stress at the front of the heat source is larger, and the transient thermal stress at the inflection point is larger than that at the middle stage.

(4) The residual stresses of the upper and lower glass layers are symmetrically distributed, and the residual stresses of the solder layer are larger than those of the glass. The process parameters have little effect on the maximum residual stresses of the edge sealing, and the maximum residual stress is about 6.46 MPa, which does not exceed 10 MPa allowed by the residual stresses of glass sealing edge.

(5) When the average laser power is 60 W and the welding speed is v=90 mm/min, the melting layer has good morphology, good mechanical properties and good welding quality, which is an optimal set of process parameters.

Acknowledgements

This research work is supported by National Natural Science Foundation of China (Grant No. 51672241), the 14th batch High-level Talents Project for “Six Talents Peak” (Grant No. XCL-092), Natural Science Foundation of Jiangsu Province (No. BK20170500), Jiangsu Science and Technology Plan Project of China (Grant No. BE2016134), the Province Postdoctoral Foundation of Jiangsu (Grant No.1501164B), the Technical Innovation Nurturing Foundation of Yangzhou University (Grant No. 2019CXJ043), China Postdoctoral Science Foundation (Grant No. 2016M600447), and Yangzhou Foundation Innovation Project (Grant No. YZ2017275, YZ2017052).

References

A. de Pablos-Martín, Th. Höche, 2017, Laser welding of glasses using a nanosecond pulsed Nd: YAG laser, Optics and Lasers in Engineering, 90, pp. 1-9.

Cao Z., Yuan Y., He G., Peterson R.L., Najafi K., 2013, Fabrication of multi-layer vertically stacked fused silica microsystems. In: Transducers & Eurosensors XXVII: The 17th International Conference on Solid-State Sensors, Actuators and Microsystems, transducers and Eurosensors, pp. 810–813.

Carter R.M., Chen J.Y., Shephard J.D., Thomson R.R., Hand D.P., 2014, Picosecond laser welding of similar and dissimilar materials. Appl Opt, 53(19), pp. 4233–8.

Faidel D., Behr W., Groß S., Reisgen U., 2010, Development of a laser-based glass sealing joining process for the fuel cell manufacturing. Phys Procedia, 5, pp. 153–62.

Fang, Y., Memon, S., Peng, J., Tyrer, M. and Ming, T., 2020. Solar thermal performance of two innovative configurations of air-vacuum layered triple glazed windows. Renewable Energy, 150, pp.167-175.

Kind H., Gehlen E., Aden M., Olowinsky A., Gillner A., 2014, Laser glass frit sealing for encapsulation of vacuum insulation glasses. Phys Procedia, 56, pp. 673–80.

Miyamoto I., Cvecek K., Schmidt M., 2011, Evaluation of nonlinear absorptivity in internal modification of bulk glass by ultrashort laser pulses. Opt Express, 19, pp. 10714–27.

Memon, S., Fang, Y. and Eames, P.C., 2019. The influence of low-temperature surface induction on evacuation, pump-out hole sealing and thermal performance of composite edge-sealed vacuum insulated glazing. Renewable energy, 135, pp.450-464.

Memon, S., 2017. Experimental measurement of hermetic edge seal's thermal conductivity for the thermal transmittance prediction of triple vacuum glazing. Case studies in thermal engineering, 10, pp.169-178.

Memon, S., Farukh, F. and Kandan, K., 2018. Effect of cavity vacuum pressure diminution on thermal performance of triple vacuum glazing. Applied Sciences, 8(9), p.1705.

Miyamoto I., Horn A., Gottmann J., Wortmann D., Yoshino F., 2007, Fusion welding of glass using femtosecond laser pulses with high-repetition rates. Journal of Laser Micro/Nanoengineering, 2, pp. 57–63.

Richter S., Zimmermann F., Eberhardt R., Tünnermann A., Nolte S., 2015, Toward laser welding of glasses without optical contacting. Appl Phys A – Mater, 121, pp. 1–9.

Shun-Yuan H.,Yu-Chia C., Jau-Sheng W., 2012, A new design of high power LED module with glass encapsulation toward high stability. In: Proceedings of the Opto-Electronics and Communications Conference (OECC), pp. 611–2.

Zhang, S.W., Zhang, J.F., Song, Y.T., Wang, Z.W., Liu, S.M., Lu, K., Chen, Z.J. and Jiang, X.P., 2011. Heat transfer and thermal stress analysis for vacuum barrier of ITER CC cryostat feed-though. Machinery Design & Manufacture, (12), pp. 194-196.

Zhang, S., Song, Y., Lu K., Wang Z., Zhang, J. and Qin, Y., 2017. Thermal analysis of the cryostat feed through for the ITER Tokamak TF feeder. Plasma Science and Technology, 19(4), pp.045601.

Zhang, S., Song, Y., Wang, Z., Lu S., Ji, X., Du, S., Liu, X., Feng, C., Yang H., Wang, S., and Luo, Z., 2014. Rapid Thermal-Hydraulic Analysis and Design Optimization of ITER Upper ELM Coils. Plasma Science and Technology, 16(10), pp. 978-983.

Miao, H., Shan, X., Liu, Y., Zhang, J.F., and Wang, H.J., 2015. Sealing performance of pbo-tio2-sio2-rxoy vacuum glass solder. Journal of material heat treatment, (12), pp. 13-18.

Mahmood, T., Mian, A., Amin, M.R., Auner, G., Witte, R., Herfurth, H. and Newaz, G., 2007. Finite element modeling of transmission laser microjoining process. Journal of Materials Processing Technology, 186(1-3), pp. 37-44.

Duffle J.A., Beckman, W.A., 1980. Solar Engineering of Thermal Processes, Wiley.